IL NUOVO CIMENTO Vol. 33 C, N. 4 Luglio-Agosto 2010
DOI 10.1393/ncc/i2010-10649-2

Colloquia: TOP2010

B-tagging, leptons and missing energy in ATLAS after first data

I. van Vulpen on behalf of the ATLAS Collaboration

Nikhef, National Institute for Subatomic Physics - Science Park 105
1098 XG Amsterdam, The Netherlands

(ricevuto il 27 Luglio 2010; approvato il 27 Luglio 2010; pubblicato online il 24 Settembre 2010)

Summary. — The start-up of the Large Hadron Collider at CERN marks a new era in particle physics. This paper presents an overview of the ATLAS detector performance and first results extracted from data taken during the early LHC runs.

PACS 14.65.Ha – Top quarks.

1. – Introduction

The new frontier of particle physics, the high-energy LHC proton-proton collisions at CERN, will allow us to study nature at the smallest distance scales to date and to pursue our main goal: to search for evidence of physics beyond the Standard Model.

With the first collisions, each of the ATLAS sub-detectors follows a detailed calibration and alignment program to study the detector response to electrons, muons, photons and jets. The events used in these calibrations range from minimum bias, through well-predicted low multiplicity (di-)lepton events to more complex event topologies. This paper presents the analysis of the first data and current understanding of the detector response([1]). A first step towards a claim of a signal from new physics is to show that the detector response is also understood in more complex event topologies. With a combination of multiple high-p_T (b-)jets, isolated high-energy leptons and large missing transverse energy, the observation and detailed measurement of top quark pair production is an important milestone in the ATLAS physics program.

2. – The Inner Detector: tracking performance and b-tagging

The heart of the ATLAS detector is formed by the Inner Detector (ID): a tracking detector inside a 2 T magnetic field covering angles up to $|\eta| < 2.5$. Tracks are reconstructed using the ID's three sub-detectors: space points from the innermost pixel detector and silicon microstrip detector (SCT) complemented with information from the transition radiation tracker (TRT) that also provides information on particle identification.

([1]) All plots and results shown in this paper can be found on the ATLAS public results webpage: https://twiki.cern.ch/twiki/bin/view/Atlas/AtlasResults.

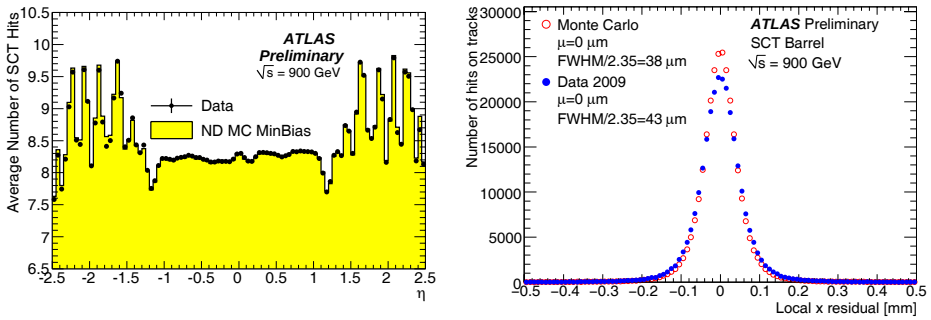

Fig. 1. – (Colour on-line) Left plot: number of SCT hits on reconstructed tracks in 900 GeV data and non-diffractive minimum bias MC simulation as a function of η. Right plot: unbiased residual distribution in x in the SCT barrel for the MC with perfect alignment (open marker) and the alignment obtained with collision data taken in 2009 (solid marker).

2˙1. *Track reconstruction.* – Basic track quantities and detector geometry are very well described by simulation. Figure 1 shows the number of SCT hits on reconstructed tracks in 900 GeV data compared to the expectation from non-diffractive minimum bias Monte Carlo (MC) simulation. Tracks were selected within $|\eta| < 2.5$, required to have a transverse momentum in excess of 500 MeV and have at least 7 SCT hits. The simulation takes into account the disabled modules in data.

A large set of well-reconstructed tracks ($p_T > 2\,\text{GeV}$, $|d_0| < 10\,\text{mm}$ and at least 6 silicon hits) allows an initial alignment of the ID by minimizing track residuals, defined as the distance between the measured hit and the prediction from the track extrapolation. Figure 1 shows the unbiased residual distribution in the x-coordinate for all hits-on-track in the SCT barrel for the MC with perfect alignment (open red) and the alignment obtained with collision data taken in 2009 (solid blue). The distributions show that the resolutions are already close to those from MC expectations.

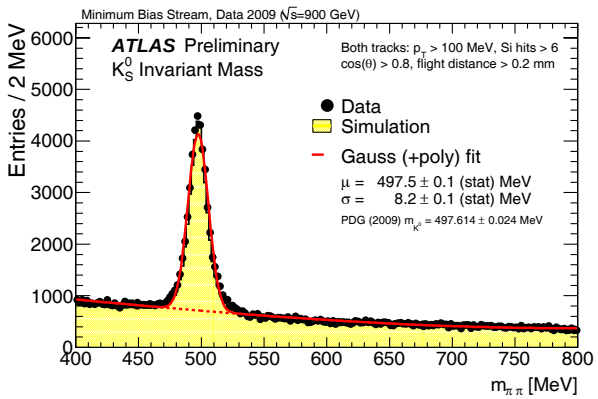

Fig. 2. – Invariant mass distribution of two-track vertices around the K_S mass.

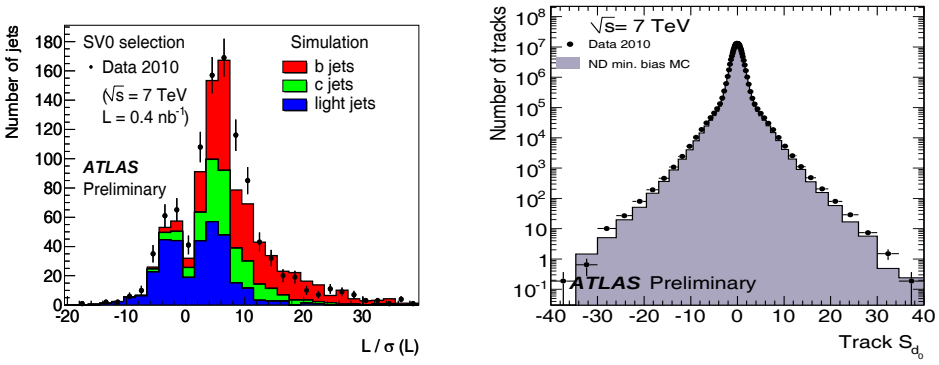

Fig. 3. – B-tagging results in 7 TeV data: transverse impact parameter significance (left plot) and the three-dimensional decay length significance (right plot).

2˙2. *Primary and secondary vertices.* – The interaction point of proton-proton collisions is reconstructed on an event-by-event basis using a dedicated primary vertex reconstruction with an efficiency close to 100%. A clear indication of the good performance and resolution of the secondary vertex tagging is shown in fig. 2 with the data to MC comparison of the K_S peak in the two-vertex-mass distribution, where the flight path of the V0 candidate is required to point back to the interaction point.

2˙3. *b-tagging.* – In ATLAS, several tagging algorithms try to identify $b(c)$-quark decays. These algorithms are based on testing a non-compatibility of the tracks associated to the jet to originate from the primary vertex and the existence (and properties) of a secondary vertex. Track quality criteria [1, 2] include the requirement to have at least 7 silicon hits. Figure 3 compares data and MC prediction for the transverse impact parameter significance d_0/σ_{d_0} for $p_T^{\text{tracks}} > 150\,\text{MeV}$ (left plot) [1] and the three-dimensional decay length significance for $p_T^{\text{tracks}} > 1\,\text{GeV}$ (right plot) [2]. The initial results on 7 TeV data as shown in the plot show an excellent understanding of the performance.

3. – Electron and muon reconstruction

The ability to reconstruct an isolated lepton with large transverse energy is a crucial step in selecting of candidates from many signals (W, Z, top quarks, new physics models) from the large number of proton-proton collisions. Both electron and muon momentum estimations use extensive information from ID tracking, but require calorimeter and TRT (electron) and the dedicated muon spectrometer information (muons) to obtain a clean identification. In this section we show a few key plots in lepton reconstruction and identification.

3˙1. *Cosmic muons.* – In the two years before LHC start-up, several hundred million cosmic muons that traversed the ATLAS detector have enabled an extensive alignment and calibration program. Figure 4 shows the transverse momentum resolution. A fit to the data (curve in plot) reveals that in the region important for top physics, *i.e.* up to 100 GeV, the resolution is close to expectation from simulation.

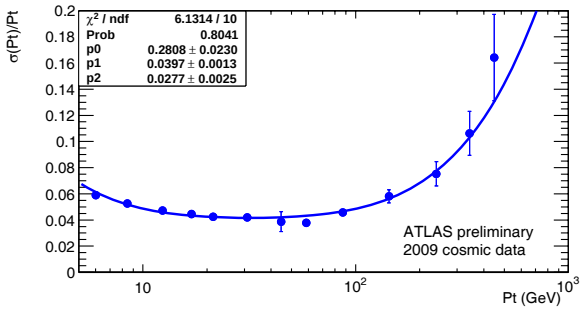

Fig. 4. – Muon transverse momentum resolution using cosmic muons.

3˙1.1. Muon reconstruction: Muons in 900 GeV data. For data taken at 900 GeV data only a few muons are expected and only 50 candidates remain after a selection that includes track quality criteria and a minimum absolute (transverse) momentum of 4 (2.5) GeV [3]. This sample is dominated by muons from π/K decays and $\sim 25\%$ are expected from semi-leptonic (b-)c-quark decays. The distributions of the pseudo-rapidity and momentum of the candidates are shown in fig. 5, where a good agreement between data and MC prediction is observed.

3˙1.2. Muon reconstruction: Muons in 7 TeV data. A well-functioning lepton trigger chain is vital for selecting interesting events from all collisions. As an indication of the muon trigger performance, the left plot of fig. 6 shows the efficiency of the Level-2 muon combined algorithm in the barrel region ($|\eta| < 1.05$) relative to the Level-2 muon spectrometer algorithm with a nominal threshold set to 4 GeV as a function of the transverse momentum of the offline reconstructed combined muon.

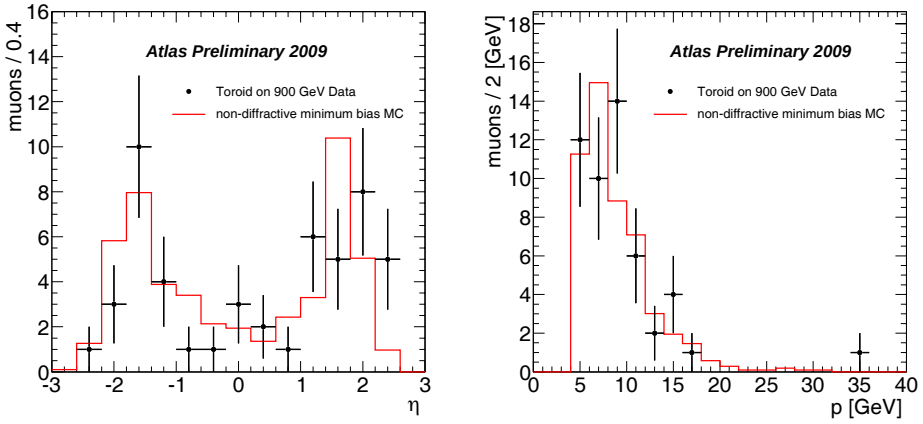

Fig. 5. – Distribution of η (left) and momentum (right) of reconstructed muons in 900 GeV data and MC. Distributions are normalized to the number of selected muon candidates. The momentum is measured by the ID reconstruction or, for combined tracks, is the result of the combined fit to the ID muon spectrometer track.

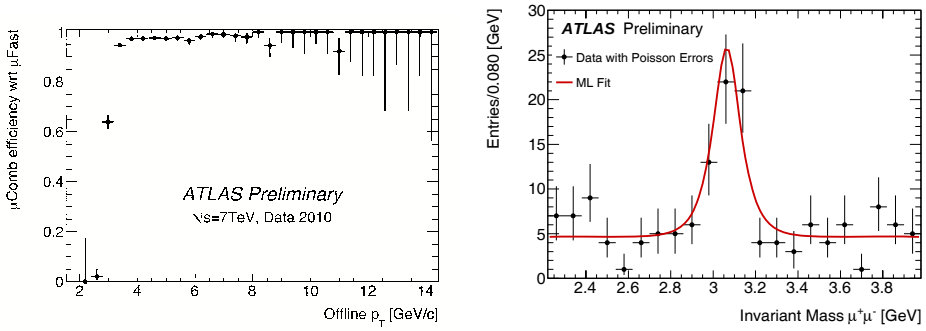

Fig. 6. – Left plot: efficiency of the L2 muon combined algorithm relative to the L2 muon spectrometer algorithm with a nominal threshold set to 4 GeV. Right plot: di-muon invariant mass distribution for $320\,\mu\mathrm{b}^{-1}$ at 7 TeV using minimum bias trigger.

Muons originating from either J/Ψ or Z-boson decays provide a clean sample of muons and, through the mass constraint, a powerful handle to assess ATLAS' capability to reconstruct muons. In the absence of a sample of Z-boson decays (we did observe a very nice $\mathrm{Z} \to \mu^+\mu^-$ candidate though), the first analyses exploit the larger statistics from J/Ψ decays. We looked for $J/\Psi \to \mu^+\mu^-$ by selecting events with two oppositely charged muons, each with a momentum above 3 GeV. The resulting mass distribution in the first $320\,\mu\mathrm{b}^{-1}$ of data at a center-of-mass energy of 7 TeV is shown in the right plot of fig. 6.

3˙2. *Electron reconstruction: Electrons in 900 GeV data.* – As for muons, in 900 GeV data only a limited number of prompt electrons are expected. We observed 879 electron candidates that are expected to originate from either photon conversions or hadrons faking an electron signature [4]. The energy in the EM calorimeter of all candidates is shown in the left plot of fig. 7. Identifying conversions using tracking information [5] allows to separate the electrons from the fakes and to test the electron reconstruction capability of ATLAS. The conversion radius from identified conversion candidates is shown in the right plot of fig. 7, showing that the material description of the ATLAS ID is accurately modeled.

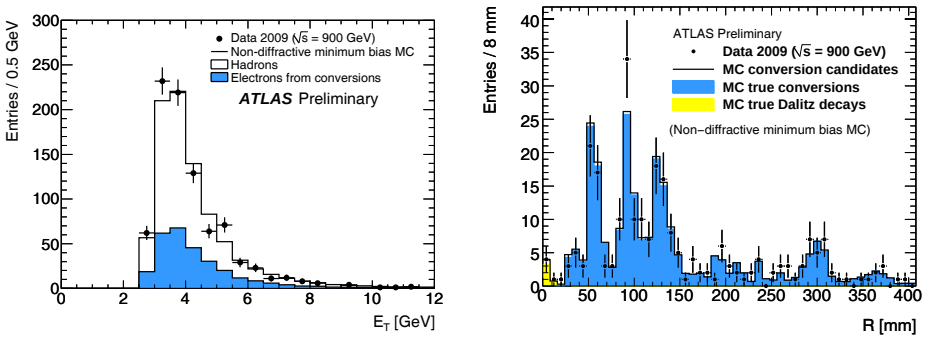

Fig. 7. – Transverse energy of the cluster for electron candidates (left) and distribution of the photon conversion radius integrated over all η for identified conversions (right).

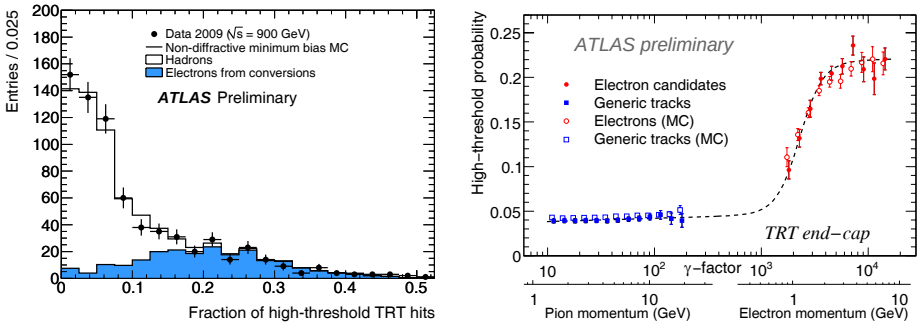

Fig. 8. – Distribution of fraction of high-threshold TRT hits for candidates with $|\eta| < 2$ (left) and the distribution of the high-threshold probability as a function of the particles Lorentz factor γ for electrons and pions separately (right).

A unique element of the ATLAS detector is the TRT. It not only provides space-points used for tracking, but is designed to provide electron-pion separation information using the (non-)detection of transition radiation that is induced by a traversing particle depending on its Lorentz factor γ. The light electrons are more likely to induce a number of high-threshold TRT hits as is shown in the left plot of fig. 8. The electron-pion separation is shown by the difference in response of the TRT to pions and electrons (from conversions) in the right plot of fig. 8.

4. – Calorimeter response and reconstructing missing transverse energy

A solid and unbiased estimate of missing transverse energy involves understanding both detector geometry and response to several physics objects to high precision. Here we present initial results based on calorimeter information [6].

4˙1. *Calorimeter response.* – The response of the electromagnetic and hadronic calorimeters at the electromagnetic (EM) scale is shown in fig. 9. The distribution of cell

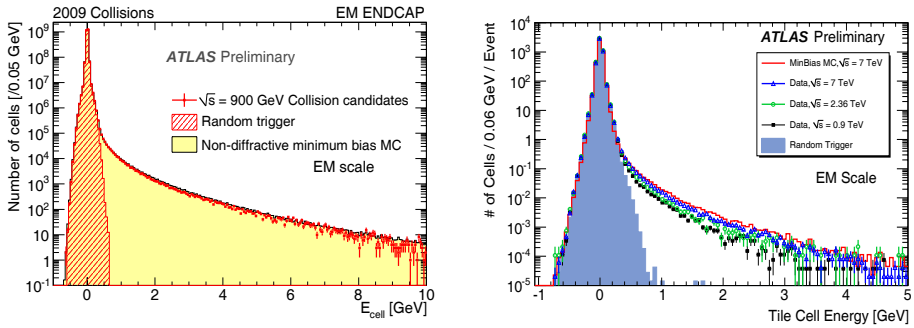

Fig. 9. – Distribution of cell energy for the electromagnetic endcap calorimeter (left plot) and the TileCal hadronic calorimeter (right plot).

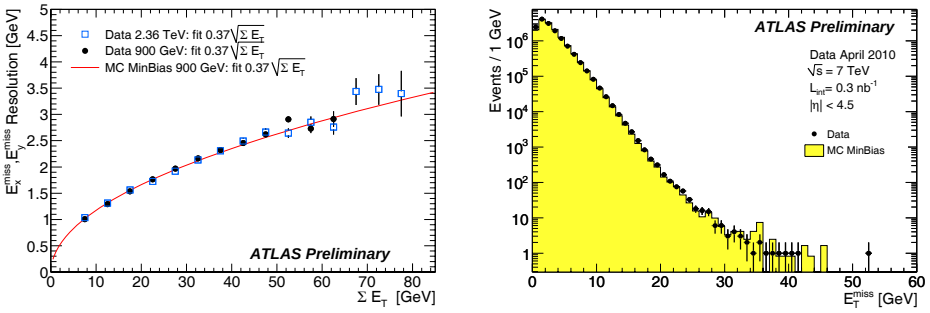

Fig. 10. – Resolution of the two components of the missing transverse energy as a function of the total sum of transverse energy in 0.9 and 2.36 TeV data (left plot) and the distribution of missing transverse energy in 7 TeV data sample compared to a normalized MC distribution (right plot).

energy([2]) in the electromagnetic calorimeter (endcap) in a run of good quality is shown in the left plot that also shows the cell energy distribution from random data (electronic noise only) as well as the expectation from non-diffractive minimum bias MC events.

The distribution of TileCal cells, a hadronic calorimeter, in collision data at 7 TeV, 2.36 TeV, and 0.9 TeV is shown in the right plot of fig. 9 where it is superimposed with Pythia minimum bias MC and randomly triggered events.

4˙2. *Missing transverse energy*. – Using topological clusters, calibrated at the EM scale, the calorimeter response can provide a first estimate of the total missing transverse energy in an event. The resolution of E_x^{miss} and E_y^{miss} as a function of the total transverse energy ($\sum E_{\mathrm{T}}$) for minimum bias events in 0.9 and 2.36 TeV data is shown in fig. 10 (left plot) [6]. The line represents a fit to the resolution obtained in the MC simulation.

The distribution of missing transverse energy in a data sample of 14.4 million selected minimum bias events at 7 TeV center-of-mass energy is shown in the right plot of fig. 10 [7]. The expectation from MC simulation is superimposed (histogram) and normalized to the number of events in data. We observe a remarkable agreement over 6 orders of magnitude and, especially important in searches for new physics, the tails seem well understood.

5. – Conclusions

The early LHC data-taking runs at 0.9, 2.36 and 7 TeV center-of-mass have allowed a first calibration, evaluation of the ATLAS detector operation and ability to reconstruct trajectories of charged particles, high-energy leptons and missing transverse energy. The agreement between data and MC on several complex physics objects like b-tagging and missing energy estimation is remarkable at this early stage. It allows us to look with confidence at more complex event topologies. We are looking forward to seeing signs of top quark pair production in the 2010 LHC runs and hopefully also hints of new physics.

([2]) Known noisy cells have been masked.

REFERENCES

[1] ATLAS Collaboration, *Tracking Studies for b-tagging with* 7 TeV *Collision Data with the ATLAS Detector*, ATLAS-CONF-2010-040 (2010).
[2] ATLAS Collaboration, *Performance of the ATLAS Secondary Vertex b-tagging Algorithm in* 7 TeV *Collision Data*, ATLAS-CONF-2010-042 (2010).
[3] ATLAS Collaboration, *Identification of muon candidates in pp collisions at* $\sqrt{s} =$ 900 GeV *with the ATLAS detector*, ATLAS-CONF-2010-015 (2010).
[4] ATLAS Collaboration, *Electron and photon reconstruction and identification in ATLAS: expected performance at high energy and results at* $\sqrt{s} = 900$ GeV, ATLAS-CONF-2010-005 (2010).
[5] ATLAS Collaboration, *Photon Conversions at* $\sqrt{s} = 900$ GeV *measured with the ATLAS Detector*, ATLAS-CONF-2010-007 (2010).
[6] ATLAS Collaboration, *Performance of the missing transverse energy reconstruction in minimum bias events at* $\sqrt{s}$ *of* 900 GeV *and* 2.36 TeV *with the ATLAS detector*, ATLAS-CONF-2010-008 (2010).
[7] ATLAS Collaboration, *Performance of the missing transverse energy reconstruction in minimum bias collisions at center-of-mass energy of* $\sqrt{s} = 7$ TeV *with the ATLAS detector*, ATLAS-CONF-2010-039 (2010).